Complete characterization of the Ar $2p_{3/2}$ photoionization via Auger-electron–photoelectron coincidence experiments

P. Bolognesi,[1] A. De Fanis,[2] M. Coreno,[1,3] and L. Avaldi[1,3,*]
[1]*CNR-IMIP, Area della Ricerca di Roma 1, CP10-00016 Monterotondo, Scalo, Italy*
[2]*Japan Synchrotron Radiation Research Institute, Sayo, Hyogo 679-5198, Japan*
[3]*INFM-TASC, Gas Phase Beamline at Elettra, Area Science Park, Basovizza, Italy*
(Received 24 February 2004; published 4 August 2004)

The photoionization of Ar $2p_{3/2}$ has been investigated by Auger electron–photoelectron coincidence experiments. The results have shown that the basic quantities that define the photoionization, i.e., the dipole matrix elements, can be extracted from these experiments and all the observables of the process, apart from the sign of the circular dichroism, can be predicted. The analysis also proved that a description of the process in terms of *LSJ* approximation is satisfactory.

DOI: 10.1103/PhysRevA.70.022701 PACS number(s): 32.80.Fb, 32.80.Hd

I. INTRODUCTION

The realization of complete experiments, where all the basic quantities, i.e., the amplitudes of the matrix elements of a particular process, are measured, is one of the main goals in atomic physics. Indeed the knowledge of these elements allows us to predict all the other observables of the process and represents the ultimate test of any theoretical description. In this work a complete description of the Ar $2p_{3/2}$ photoionization has been achieved by a set of Auger electron–photoelectron coincidence measurements.

Auger electron–photoelectron coincidence experiments have been pioneered by Haak *et al.* [1], who introduced this technique to unravel the Auger spectrum of solid Cu, and then transferred to free atoms in gas phase [2]. In these experiments the inner shell photoionization process and its nonradiative decay to the double continuum are investigated in detail. When the intermediate state corresponds to a well-defined isolated resonance in the double ionization continuum, the competing direct double ionization is negligible and the lifetime of the intermediate state is long enough to prevent any final state interaction then the process can be considered a sequential one, consisting of two incoherent steps. In such a case Auger electron–photoelectron coincidence experiments are a suitable tool to achieve (i) a better and unambiguous spectroscopic characterization of the emitted electron spectra [2] and (ii) a deep insight into the two constituent processes [3–5]. Indeed this kind of experiment has been proposed as "complete experiments" [6] where the photoionization dipole matrix elements can be obtained experimentally. However, in previous work [3–5] coincidence data have always been combined with the results of noncoincidence experiments to obtain the "complete" information on the process. Here, following the theoretical suggestions of Kabachnik [6] only coincidence data are used to obtain the values of the amplitudes and then to predict all the other observables that characterize the process.

*Email address: lorenzo.avaldi@imip.cnr.it

II. EXPERIMENT

The experiment has been performed at the Gas Phase beamline of the Elettra storage ring using the multicoincidence end-station [7]. Detailed descriptions of the beamline, the experimental station, and experimental procedures have been given elsewhere [7]. The experimental station hosts ten hemispherical electron energy analyzers mounted on two independent turntables. Seven of these are on a larger frame and placed at 30° angular intervals on a turntable that can rotate in the plane perpendicular to the direction of propagation of the incident radiation. The other three analyzers are mounted on a smaller turntable at 0°, 30°, and 60° with respect to the polarization vector of the light. This second turntable can be rotated around the polarization vector. In these measurements both arrays have been kept in the perpendicular plane. The energy resolution in the present experiment was about 80 and 200 meV for the detection of the photoelectrons and the Auger electrons, respectively. The angular acceptance in the dispersion plane of the spectrometers was ±3°. The overall energy resolution was sufficient to separate the L_2 and L_3 Auger components in the coincidence experiment, but not enough to resolve the spin–orbit structure of the final Auger state. In the experiment the signals of each of the three analyzers of the small turntable are used as "starts" and the signals from the other seven as "stops" in the coincidence electronics. In this way 21 coincidence pairs are collected simultaneously. The angular distribution is obtained by successive rotations of the larger frame.

The experiment has been performed at the photon energy $h\nu = 253.6$ eV, i.e., 5 eV above the Ar L_3 threshold. The relative efficiency of the analyzers has been calibrated via the measurement of the photoelectron angular distribution of the $He^+(n=3)$ and of the $Xe^+(4d^9)$ states at 5 and 200 eV above their respective thresholds [8,9] and checked in the angular distribution of the $He^+(1s)$ state. Then the same efficiency correction has been assumed for the coincidence measurements. All the data are internormalized and therefore each set of the experimental coincidence angular correlations is reported on a common scale of counts.

III. RESULTS AND DISCUSSION

The processes investigated are the Ar $2p_{3/2}$ photoionization and the following decays of the $2p_{3/2}$ hole:

$$h\nu + \mathrm{Ar} \rightarrow \mathrm{Ar}^{+}2p_{3/2}^{5}\left(^{2}P_{3/2}^{o}\right) + e_{ph}(\varepsilon s_{1/2}, \varepsilon d_{3/2}, \varepsilon d_{5/2})$$

$$\rightarrow \mathrm{Ar}^{2+}3p^{4}\left(^{1}S_{0}^{e}\right) + e_{\mathrm{Auger}}(\varepsilon p_{3/2}) \tag{1a}$$

$$\rightarrow \mathrm{Ar}^{2+}3p^{4}(^{1}D_{2}^{e}) + e_{\mathrm{Auger}}(\varepsilon p_{1/2}, \varepsilon p_{3/2}, \varepsilon f_{5/2}, \varepsilon f_{7/2}) \tag{1b}$$

$$\rightarrow \mathrm{Ar}^{2+}3p^{4}(^{3}P_{0,1,2}^{e}) + e_{\mathrm{Auger}}(\varepsilon p_{1/2}, \varepsilon p_{3/2}). \tag{1c}$$

The angular distribution of the $L_3M_{23}M_{23}$ Auger electrons has been measured in coincidence with a photoelectron detected at fixed directions. In the case of the Ar^{2+} ($^1S_0^e$) final state the complementary experiment, in which the angular distribution of the 5 eV photoelectron is measured in coincidence with the $L_3M_{23}M_{23}$ ($^1S_0^e$) Auger electron detected at a fixed direction, has been performed too.

The basic quantities to describe the Ar $2p_{3/2}$ photoionization in the dipole approximation are the three dipole matrix elements $D_j = \langle 2p^6\ ^1S \| \mathbf{d} \| 2p^5\ ^2P_{3/2}\varepsilon_{lj}\rangle = |D_j| e^{-i\Delta j}$ with $l=0$, $j=1/2$, and $l=2$ $j=3/2,5/2$. An absolute phase is irrelevant, so we shall consider only two independent phase differences $\Delta_{ij} = \Delta_i - \Delta_j$. Thus the quantities that fully characterize this process are five. In order to achieve a complete description of the photoionization, previous experiments used either the cross section σ, the β parameter, and the three spin-polarization parameters, ξ, η, and ζ, of the photoelectrons [10]; or the cross section σ, the β parameter, of the photoelectrons, the alignment A_{20} of the photoion, and a set of parameters from the representation [3] of the Auger-photoelectron coincidence angular correlation [11,12]. At variance, in the present work only the coincidence angular correlation has been used. This has been described by the general expression derived using the density matrix and statistical tensor formalism by Kabachnik [6]. The amplitudes $|D_j|$ and relative phases Δ_{ij} of the dipole matrix elements are contained in this general expression and therefore these are the quantities used as free parameters in the fit to the data.

In the two step approximation the coincidence angular correlation, which is represented by the triple differential cross section (TDCS) $d^3\sigma/d\Omega_1\, d\Omega_2\, dE_1$, is given by an expression [6], which disentangles the properties of the light polarization, the geometry of the two electron emission, and the dynamical parameters

$$d^3\sigma/d\Omega_1\, d\Omega_2\, dE_1 \propto \rho_{00}(J, \vartheta_1, \varphi_1)\Bigg[1 + \sum_{k_2>0,even} \alpha_{k_2} \sum_{q_2} A_{k_2q_2}(J, \vartheta_1, \varphi_1) \times \sqrt{\frac{4\pi}{2k_2+1}} Y_{k_2q_2}(\vartheta_2, \varphi_2)\Bigg], \tag{2}$$

where labels 1 and 2 refer to the photoelectron and Auger electron respectively, ρ_{00} describes the angle-dependent intensity for the noncoincident observation of the photoelectron, α_{k_2} are the Auger anisotropy coefficients [13], $A_{k_2q_2}$ the alignment tensor which describes the ionic state J produced by the inner shell photoionization with the photoelectron detected in the direction (ϑ_1, φ_1), and $Y_{k_2q_2}$the spherical harmonics. In the Ar $2p_{3/2}$ photoionization [6] with linearly polarized radiation, both electrons detected in the perpendicular geometry, and considering the case of the Ar^{2+} ($^1S_0^e$) final state, where part of the Auger decay reduces to a known numerical value (i.e., $\alpha_2 = -1$) [6], the TDCS becomes

$$d^3\sigma/d\Omega_1\, d\Omega_2\, dE_1 \propto \rho_{00}\left(\frac{3}{2}, \vartheta_1\right)\Bigg[1 - \sqrt{\frac{4\pi}{5}} \sum_{q_2} A_{2q_2} \times \left(\frac{3}{2}, \vartheta_1\right) Y_{2q_2}(\vartheta_2)\Bigg]. \tag{3}$$

The magnitudes $|D_j|$ of the dipole matrix elements and their relative phases Δ_{ij} enter in the expressions of the A_{2q_2} statistical tensors [6]. The Δ_{ij} appear only via the cosine function, thus the sign of these phases remains undetermined. Conditions for the validity of the two step approximation are that the two electrons are distinguishable, which is the case in the present experiment because they have different energies, and postcollision interaction (PCI) is negligible. The shift in energy due to PCI has been taken into account in the experiment by tuning the analyzers to the peak of the photoelectron line shape. As for the PCI effects in the angular correlation it has been shown [14] that they become relevant when the two electrons have almost the same energy and they are detected at a small relative angle. None of these conditions occurs in this work, thus these effects have been neglected.

The measured TDCSs relative to process (1a) are shown in Fig. 1. Only the TDCS measured at $\vartheta_1 = 0°$, i.e., with the photoelectron detected along the polarization axis of the incident radiation, displays a cylindrical symmetry around the direction of polarization. For the other two TDCSs neither the direction of the photoelectron nor the axis of polarization of the incident radiation represents an axis of symmetry.

Formula (3) has been used in a simultaneous fit of the three sets of data at different ϑ_1. As already discussed by previous work [11,12] the dipole matrix elements D_j in formula (3) present strong statistical correlation. Thus the extraction of their values from the fit is not straightforward. The use of three internormalized TDCSs provides the advantage to sample a larger region of the multidimensional space of the fitting parameters. In the fitting we have written formula (3) in terms of the amplitude ratios $|D_{1/2}/D_{3/2}|$ and

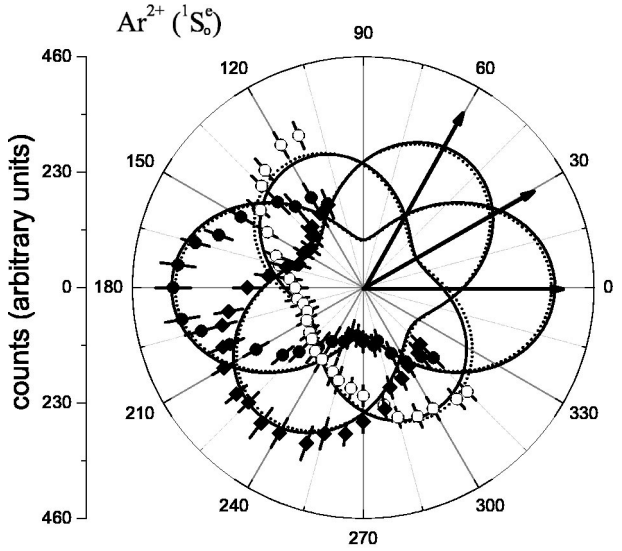

FIG. 1. Auger-electron–photoelectron coincidence angular correlations for the Ar^{2+} ($^1S_0^e$) state. The photoelectron was detected at $\vartheta_1=0°$ (dots), 30° (lozenges), and 60° (open circles), respectively. The curves are the result of a simultaneous fit to the three sets of data using formula (3) with the *LSJ* constraints (solid line) or without any constraints (dashed line).

$|D_{5/2}/D_{3/2}|$ (because in this experiment no absolute values are measured), phase differences $\Delta_{1/2-3/2}$ and $\Delta_{5/2-3/2}$, and a scaling factor. In this way the number of free parameters is reduced to five. First we worked in the *LSJ* approximation and neglected the spin–orbit interaction in the continuum, i.e., $|D_{5/2}/D_{3/2}|=3$ and $\Delta_{5/2-3/2}=0$ [15]. The results of this fit are represented by the full lines in Fig. 1. Next we removed the above mentioned constraints and repeated the fit. In this latter case it should be noted that, depending on the initial guess of the parameters, it is possible to achieve almost equivalent fits of the experimental data, according to statistical tests, with values of the phases $\Delta_{1/2-3/2}$ and $\Delta_{5/2-3/2}$ which differ more than their uncertainties. We selected the set of parameters with the lowest χ^2 value. These parameters, which produce the dashed curves of Fig. 1, are reported in Table I and compared with the ones obtained from the LSJ approximation. The results of the two procedures are consistent, but the parameters obtained without the *LSJ* constraints are characterized by larger uncertainties. The TDCSs calculated with the two sets of parameters are practically undistinguishable (Fig. 1) and give a reasonable representation of the data. This analysis leads to the conclusion that the *LSJ* approximation is sufficient for the description of the Ar $2p_{3/2}$ photoionization. Therefore we have analyzed the TDCS of the other two channels using the results of the fit in the *LSJ* approximation.

TABLE I. Amplitudes and relative phases obtained in the fit with and without the constraints of the *LSJ* approximation to the $L_3M_{23}M_{23}$ ($^1S_0^e$) Auger electron–photoelectron angular correlations. The values in the last row are the reduced χ^2.

	LSJ	*jj*
$\lvert D_{1/2}/D_{3/2}\rvert$	1.85±0.10	1.77±0.13
$\lvert D_{5/2}/D_{3/2}\rvert$	3	2.60±0.25
$\Delta_{1/2,3/2}$	62°±2°	62°±13°
$\Delta_{3/2,5/2}$	0°	0°±13°
χ^2	1.2	1.3

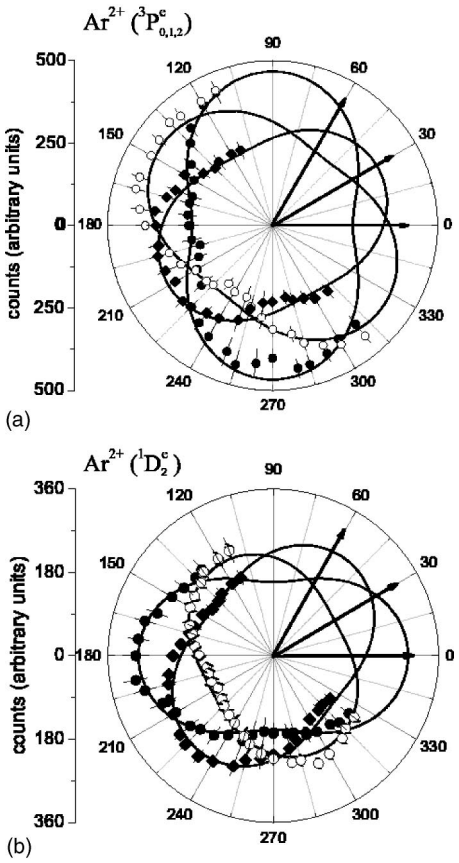

FIG. 2. Auger-electron–photoelectron coincidence angular correlations for the Ar^{2+} ($^3P_{0,1,2}^e$) (a) and ($^1D_2^e$) (b) states. The photoelectron was detected at $\vartheta_1=0°$ (dots), 30° (lozenges), and 60° (open circles), respectively. The curves are the result of the simultaneous fit of the three sets of data for each final state using the amplitudes and relative phases obtained in the Ar^{2+} ($^1S_0^e$) case.

The other two decay channels of the Ar^+ $2p_{3/2}^{-1}$ vacancy represented by reactions (1b) and (1c) are characterized by the same matrix elements of the photoionization process as Eq. (1a). The α_2 Auger parameter will be different depending on the final Ar^{2+} ion state. Thus in the fits of the TDCSs for channels (1b) and (1c) the values of D_j have been kept fixed to those extracted from channel (1a), and only α_2 was left as free parameter. The results are shown in Figs. 2(a) and 2(b) for the Ar^{2+} ($^3P_{0,1,2}^e$) and ($^1D_2^e$) final states, respectively. A satisfactory representation of the data is obtained in both cases. The α_2 values obtained from the fit are compared in Table II with previous determinations in an ion impact experiment [16] and from theoretical predictions [17]. A good agreement exists between the two experimental determinations, while a too large value is predicted by theory in the case of the $^3P^e$ ion state.

The D_j values have then been used to calculate the complementary TDCS, where the $L_3M_{23}M_{23}$ ($^1S_0^e$) Auger

TABLE II. The anisotropy coefficients α_2 of the Auger electrons emitted in the decay of the $2p_{3/2}$ hole to the Ar^{2+} ($^3P^e_{0,1,2}$) and ($^1D^e_2$) states.

	α_2		
	This work	Sarkadi *et al.*[a]	Kabachnik *et al.*[b]
($^3P^e_{0,1,2}$)	0.38±0.02	0.37±0.1	0.48
($^1D^e_2$)	−0.44±0.02	−0.48±0.1	−0.44

[a]Reference [16].
[b]Reference [17].

electron is detected at $\vartheta_2=30°$ and the photoelectron angular distribution is measured in coincidence with this Auger electron (Fig. 3). Despite the error bars being larger than in the other TDCS, the shape of the TDCS is definitely different from the noncoincidence angular distribution of the photoelectrons. The TDCS, calculated using the values of the amplitudes of Table I and only a scaling factor as a free parameter, is in reasonable agreement with the experiment.

The other observables in a photoionization experiment are the asymmetry parameter β of the photoelectrons, the alignment A_{20}, and the orientation A_{10} of the photoion, and the ξ, η, and ζ spin polarization parameters of the photoelectrons [18]. All these quantities, calculated from the values of the parameters of Table I, are collected in Table III where they are compared with previous experimental determinations [19–21] and theoretical predictions [19,22]. The only observable which cannot be derived from this set of data is the sign

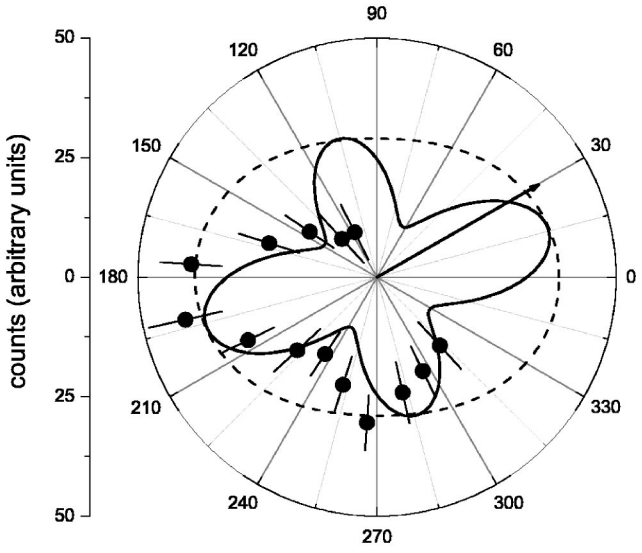

FIG. 3. Angular correlation between the photoelectron and an Auger electron detected at $\vartheta_2=30°$ (dots) for the Ar^{2+} ($^1S^e_0$) state. The curves represent the prediction of formula (3) using the amplitudes and relative phases from the fit to the complementary TDCS (solid line) and the noncoincidence angular distribution of the photoelectrons (dashed line), respectively.

TABLE III. Values of the observables of Ar $2p_{3/2}$ photoionization calculated with the amplitudes obtained in *LSJ* approximation. A_{20} has been derived assuming as a reference axis the direction of polarization of the incident radiation, while A_{10} has been calculated assuming a radiation fully circularly polarized.

	This work	Previous experiments	Theory
β_{ph}	0.17±0.06	0.24±0.06[a]	0.32[a]
		0.19±0.03[b]	0.6[d]
A_{20}	0.32±0.02	0.27±0.1[c]	0.15[c]
			0.12[e]
A_{10}	−0.13±0.05		−0.53[e]
ξ	−0.53±0.02		
η	−0.36±0.01		
ζ	−0.72±0.02		

[a]See Ref. [19].
[b]See Ref. [20].
[c]See Ref. [21].
[d]See Ref. [24].
[e]See Ref. [22].

of the circular dichroism, which can be measured in experiments with circularly polarized radiation.

Finally the $|D_j|$ can be placed on an absolute scale using their relationship with the partial photoionization cross section

$$\sigma(2p_{3/2}) = \frac{4\pi^2}{3}\alpha h\nu(|D_{1/2}|^2 + |D_{3/2}|^2 + |D_{5/2}|^2), \qquad (4)$$

where α is the fine structure constant. Using the Ar $2p$ absolute photoionization cross section by Deslattes [23] and the $2p_{1/2}/2p_{3/2}$ branching ratio [24] we found $|D_{1/2}|=0.18\pm0.01$ a.u., $|D_{3/2}|=0.096\pm0.01$ a.u., and $|D_{5/2}|=0.29\pm0.02$ a.u. A complete description of Ar $2p$ photoionization was attempted previously [21] via the measurements of noncoincidence angular distributions of photoelectrons and $L_3M_{23}M_{23}$ ($^1S^e_0$) Auger electrons in the framework of the LS approximation. The absolute values of matrix elements of the present work, when properly recoupled to give the D_s and D_d matrix elements used in the LS approximation, are in good agreement with the values derived in that work and the present value of $\Delta_{1/2-3/2}$ is consistent with the phase difference of about 51° there determined.

In summary, in this work an Auger electron–photoelectron coincidence experiment has allowed us to obtain all the basic quantities needed to describe the Ar $2p_{3/2}$ photoionization process at 5 eV above threshold. The present results, consistent with a previous analysis [21], prove that the LSJ approximation is sufficient to describe this process.

ACKNOWLEDGMENTS

The authors are indebted to N. Kabachnik for useful discussions and suggestions and to U. Kleiman for sending the results of his calculations in tabular form.

[1] H. W. Haak, G. A. Sawatzky, and T. D. Thomas, Phys. Rev. Lett. **41**, 1825 (1978).
[2] E. von Raven, M. Meyer, M. Pahle, and B. Sonntag, J. Electron Spectrosc. Relat. Phenom. **52**, 677 (1990).
[3] B. Kämmerling and V. Schmidt, Phys. Rev. Lett. **67**, 1848 (1991); **69**, 1145 (1992).
[4] A. De Fanis *et al.*, J. Phys. B **32**, 5739 (1999).
[5] A. De Fanis, H.-J. Beyer, K. J. Ross, and J. B. West, J. Phys. B **34**, L99 (2001).
[6] N. M. Kabachnik, J. Phys. B **25**, L389 (1992).
[7] R. R. Blyth *et al.*, J. Electron Spectrosc. Relat. Phenom. **101–103**, 959 (1999).
[8] R. Wehlitz *et al.*, J. Phys. B **26**, L783 (1993).
[9] D. W. Lindle, T. A. Ferrett, P. A. Heimann, and D. A. Shirley, Phys. Rev. A **37**, 3808 (1988).
[10] F. Schäfers, G. Schönense, and U. Heinzmann, Phys. Rev. A **28**, 802 (1983); N. Müller *et al.*, J. Electron Spectrosc. Relat. Phenom. **72**, 187 (1995).
[11] B. Kämmerling and V. Schmidt, J. Phys. B **26**, 1141 (1993).
[12] S. J. Schaphorst *et al.*, J. Phys. B **30**, 4003 (1997).
[13] N. M. Kabachnik and I. P. Sazhina, J. Phys. B **17**, 1335 (1984).
[14] S. A. Sheinerman and V. Schmidt, J. Phys. B **30**, 1677 (1997).
[15] U. Heinzmann, J. Phys. B **13**, 4353 (1980).
[16] L. Sarkadi *et al.*, J. Phys. B **23**, 3643 (1990).
[17] N. M. Kabachnik, B. Lohmann, and W. Mehlorn, J. Phys. B **24**, 2249 (1991).
[18] K.-N. Huang, Phys. Rev. A **22**, 223 (1980).
[19] D. W. Lindle *et al.*, Phys. Rev. A **31**, 714 (1985).
[20] L. Avaldi *et al.*, J. Phys. B **27**, 3953 (1994).
[21] U. Becker and B. Langer, Phys. Scr., T **78**, 13 (1998); U. Becker, J. Electron Spectrosc. Relat. Phenom. **96**, 105 (1998).
[22] U. Kleiman and B. Lohmann, J. Electron Spectrosc. Relat. Phenom. **131–132**, 29 (2003).
[23] R. D. Deslattes, Phys. Rev. **186**, 1 (1969).
[24] M. Kutzner, Q. Shamblin, S. E. Vance, and D. Winn, Phys. Rev. A **55**, 248 (1997).